Anisotropy of the transport critical current in (110)-, (113)-, and a-axis-oriented $YBa_2Cu_3O_{7-\delta}$ thin films

J. Z. Wu and W. K. Chu

Texas Center for Superconductivity and Department of Physics, University of Houston, Houston, Texas 77204-5932

(Received 16 April 1993; revised manuscript received 29 June 1993)

The transport critical currents of (110)-, (113)-, and a-axis-oriented $YBa_2Cu_3O_{7-\delta}$ thin films were measured as a function of the magnetic-field direction at different temperatures (4.2–77 K) and magnetic fields (≤ 1.5 T). Major peaks due to the intrinsic pinning were observed when the magnetic field was parallel to the Cu-O planes while secondary peaks due to surface pinning were only seen at high temperatures. The temperature dependence of J_c shows different behavior in these thin films. Possible reasons for this are discussed.

I. INTRODUCTION

It is important to study the anisotropic behavior of the transport critical current density (J_c) in high-temperature superconductors (HTS) as a direct probe to various pinning mechanisms. Knowledge of this issue is limited and ambiguous though much effort has been made.[1–4] The difficulty with this investigation is that J_c depends on both intrinsic and extrinsic factors introduced during the fabrication of the material. In the measurement of $J_c(\theta)$ (see Fig. 1) along the Cu-O planes (ab plane) of $YBa_2Cu_3O_{7-\delta}$ (YBCO) single-crystal bulk or c-axis-oriented thin films, all studies show a pair of J_c peaks at $\theta=\pm 90°$, when the magnetic field (H) is parallel to the Cu-O planes. But different theoretical fits[1,2] of this angular dependence are reported. It is unclear whether YBCO can be described as an ideal anisotropic superconductor as defined by the Ginsburg-Landau theory[5] or as a two-dimensional superconducting layered structure as implied by the intrinsic pinning model.[6] Moreover, another pair of J_c peaks at $\theta=0°$ or 180° as H is parallel to the twin boundary were observed on c-axis-oriented YBCO thin films in certain temperature (T) and field range.[4] It seems plausible to attribute it to the twin-boundary pinning effect but, on the other hand, it is hard to understand why this effect has not been observed in twinned single-crystal bulk samples.[7] In c-axis-oriented YBCO thin films, the Cu-O planes are parallel to the surface. It is thus difficult to separate the surface pinning from the strong intrinsic pinning in these films.[4]

In this paper, we report J_c measurements on (110)-, (113)-, and a-axis-oriented YBCO thin films. Different types of growth defects are introduced as the orientation of the YBCO thin films changes. The study of the J_c anisotropy in these films provides information on both intrinsic and extrinsic pinning mechanisms. In particular, since the Cu-O planes are no longer coplanar with the surface and film-substrate interface, the surface-pinning effect can be studied independently from the strong intrinsic pinning.

II. SAMPLE PREPARATION

YBCO thin films were prepared by the pulsed-laser ablation technique using an excimer laser ($\lambda=248$ nm). The energy density of each laser pulse was estimated to be 1–2 J/cm^2. The distance between the target and the substrate was around 3.5 cm and the deposition rate is about 1 Å/sec. The orientation of the YBCO thin films is controlled by the deposition temperature (T_s) and oxygen pressure (P_{O_2}) as previously discussed.[8] The deposition parameters are listed in Table I. The substrates were affixed to the heater by silver paste to obtain good thermal contact. T_s is measured with an Omega inconnel-sheathed K-type thermocouple embedded in a small hole drilled parallel to and underneath the heater surface. The fluctuation of T_s is within ± 2 K. For the c-axis and (113) orientations, the substrate was preheated to T_s in 10 min followed by the deposition at T_s. For the a-axis or (110) orientations, a two-step deposition pro-

TABLE I. Deposition parameters for YBCO thin films of different orientations.

Orientation	c	a	(110)	(113)
Substrate	(100) $SrTiO_3$ (100) $LaAlO_3$ (100) MgO	(100) $SrTiO_3$ (100) $LaAlO_3$	(110) $SrTiO_3$	(111) $SrTiO_3$
T_s (C)[a]	740–750	670–690	660–690	740–750
P_{O_2} (mTorr)	180–200	160–180	160–180	180–200
T_{anneal} (C)	450	510	510	450
t_{anneal} (min)	30	40	40	30

[a] T_s for (110)- and a-axis-oriented films is for the first step.

TABLE II. Basic features of YBCO thin-film samples used in this experiment.

	Sample 1	Sample 2	Sample 3	Sample 4	Sample 5	Sample 6
Orientation	(110)	(110)	*a*	*a*	(113)	(113)
Phase purity[a]	99%	99%	99%	99%	N/A	N/A
T_c (K)	84.0	86.7	83.7	82.2	89.5	90.1
Thickness (Å)	1500	1900	1500	1300	1000	1200
Current direction	[110],*c*	[110],*c*	[013]	*c* or *b*	$[1\bar{1}0]$	$[11\bar{6}]$
ρ_1 (300 K)[b] (mΩ cm)	0.23	0.22	0.52	0.55	0.49	0.51
ρ_2 (300 K) (mΩ cm)	5.1	4.8	0.56	0.53	0.48	0.51
$d\rho_1/dT$ (mΩ cm/K)	2.4	2.6	2.0	1.9	2.6	2.8
$d\rho_2/dT$ (mΩ cm/K)	N/A	N/A	2.0	1.9	2.6	2.75

[a]Impurity phase for (110) thin films is mostly (103)-oriented YBCO; and for *a*-axis-oriented thin films, *c*-axis-oriented YBCO.
[b]In (110) films, line 1 refers to the *ab* plane and line 2, the *c* axis.

cedure[9] was adopted to achieve good superconductivity and high phase-purity of single orientation. A thin YBCO or $PrBa_2Cu_3O_{7-\delta}$ buffer layer with thickness of 100–300 Å was first deposited at 650–660 °C. After the first deposition, T_s was increased to 700–740 °C in 2–3 min and the second deposition of YBCO followed. After deposition, the heater temperature was decreased quickly to 600 °C, and 300 Torr O_2 was introduced into the chamber. The samples were then cooled slowly to the annealing temperature T_a and annealed for $t_a \sim 30$ min.

The orientation of the films was checked by x-ray diffraction. As discussed in Ref. 8, both *a*-axis and *c*-axis-oriented YBCO phases can be grown on (100) $SrTiO_3$ or $LaAlO_3$ substrates while (110)- and (103)-oriented YBCO phases, on (110) $SrTiO_3$ substrates. The volume percentage of the *a*-axis and *c*-axis-phases was generally estimated by the ratio of the (200) and (005) peak intensities in the normal $\theta-2\theta$ scan, and the volume percentage of the (110) and (103) phases was calculated by the intensities of (108) peak in (108)-Φ scan.[8] The surface morphology of the films was studied by scanning electron microscopy. Generally, the (110)- and *a*-axis-oriented YBCO thin films had smoother and crack-free surfaces.

A pair of microbridges was patterned photolithographically followed by Ar-ion milling. On YBCO (110) thin films, the two bridges are perpendicular to each other with one along the *ab* plane and the other along the *c* axis. On all the other YBCO thin films, two parallel bridges were prepared. The bridges were 10 or 20 μm wide and 1 mm long. Ozone treatment after the patterning was adopted to improve the surface condition. Silver contact dots of 400–600 Å thick were sputtered, either before or after the patterning, on thin films through a metal mask. Samples are further annealed at 500 °C and 300 Torr O_2 for 1 h to achieve good electrical contacts. The transition temperature T_c was checked before patterning by the ac method to avoid contamination of the surface and after, by the standard four-point method. Caution was taken in patterning processing to avoid the degradation of the superconductivity. Many samples were measured with consistent results. In Table II, we list the basic features of six samples after the patterning. J_c was then determined by the criterion 0.8 μV/1 mm from the *I-V* curve in a dc measurement.

III. EXPERIMENTAL RESULTS

In the setup shown in Fig. 1, J_c can be measured as functions of θ, T, and H. J is held perpendicular to H during the measurement. T is monitored by a Au-Fe vs chromel thermocouple glued on the back of the sample by silicone. During the measurement, T is controlled within ±0.1 K in the temperature range (10–300 K) with an Oxford TC4 temperature controller. Resolutions of θ and H are 1° and 0.01 T, respectively.

A. Angular dependence

$J_c(\theta)$'s of YBCO thin films of various orientations are displayed at $T=20$ K and $H=1.5T$ (see Fig. 2). For (110)-oriented YBCO thin films, J was passed along the *ab* plane ([110] axis) and *c* axis, respectively [see Fig. 2(a)]. When J is along the *ab* plane [Fig. 2(ai)], two J_c peaks are located at $\theta=0°$ and ±180° where H is parallel to the Cu-O planes. The lowest J_c is found at $\theta=\pm 90°$ where H is perpendicular to the Cu-O planes. The peak-to-valley ratio of J_c is about 2.4 which is close to that observed on *c*-axis-oriented YBCO thin films.[4] We have attempted to fit the experimental data to the effective-mass[5] model and the intrinsic-pinning[6] model, respectively. A better fit is obtained with the latter [Fig. 2(ai), solid line] which indicates that the anisotropy of J_c is caused primarily by the anisotropy of the pinning effect. When J flows along the *c* axis [Fig. 2(aii)], no variation of J_c has been observed as expected since H is always parallel to the *ab* plane. Meanwhile it implies that other pinning effects, such as the growth-defects pinning, are minor and

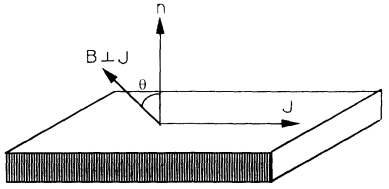

FIG. 1. Schematic description of $J_c(\theta)$ measurement in the magnetic field. θ is the angle between H and the normal of the film. J is held perpendicular to H during the measurement.

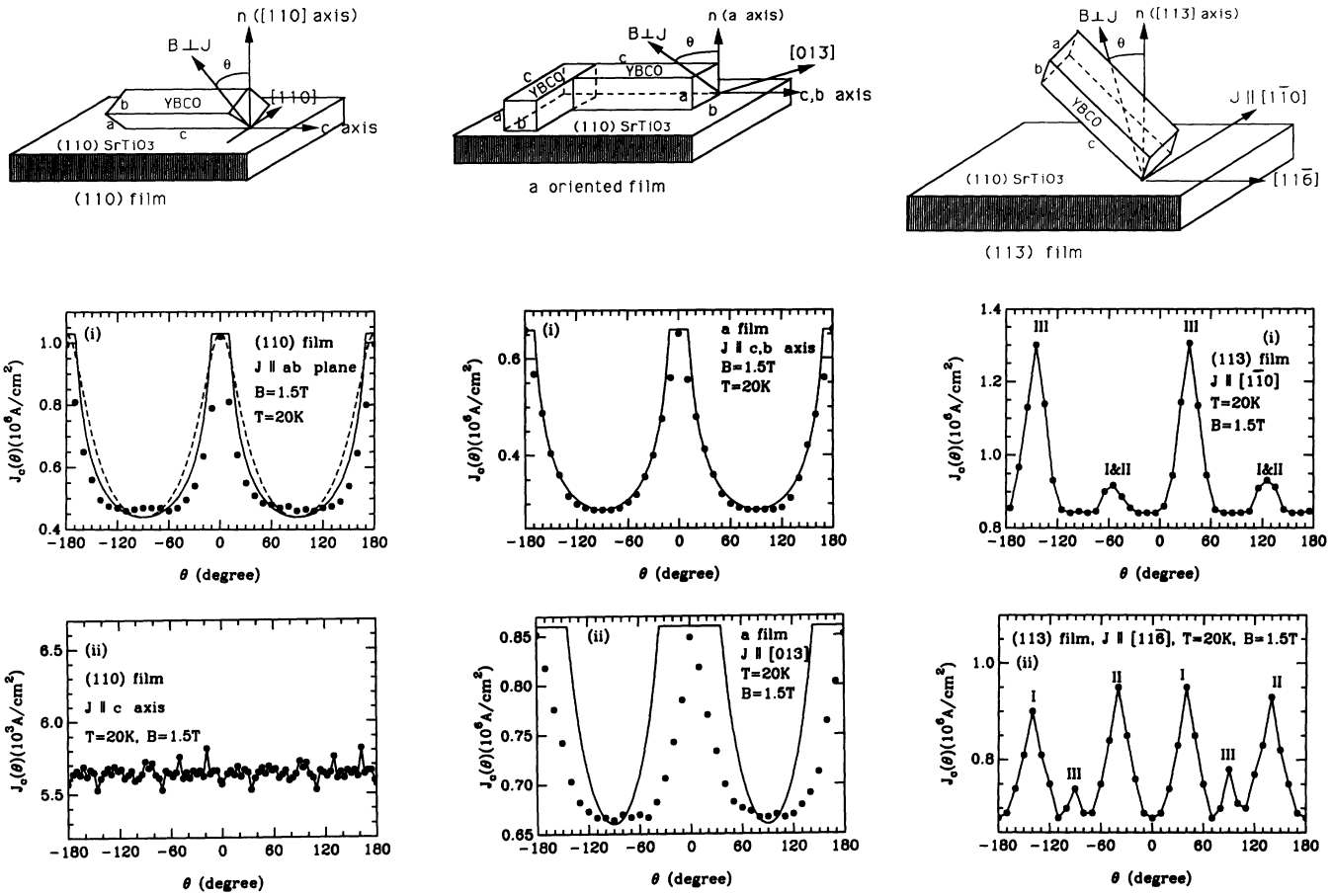

FIG. 2. $J_c(\theta)$ of YBCO thin films of different orientations. (a) (110)-oriented thin films as J is (i) along the ab plane and (ii) c-axis; (b) a-axis-oriented thin films as J is along (i) the c or b axis and (ii) [013] axis; and (c) (113)-oriented thin films as J is along (i) the [1$\bar{1}$0] axis and (ii) [11$\bar{6}$] axis. Solid line is from the intrinsic-pinning model and dashed line, the effective-mass model where $J_c(\theta) \sim H_{c2}(\theta)$. H is 1.5 T and T is 20 K.

have no visible anisotropy in (110)-oriented YBCO thin films.

$J_c(\theta)$ in a-axis-oriented YBCO thin films is similar to that of (110)-oriented YBCO thin films since the Cu-O planes are perpendicular to the film surface in both cases. Unlike (110)-oriented films, a-axis-oriented films generally consist of two kinds of microdomains. The Cu-O planes in these microdomains are perpendicular to each other. To understand how the J_c anisotropy is influenced by the direction of J with respect to these domains, we passed J along two different directions. One is along the c axis (or b axis) where J is parallel to the Cu-O planes in one group of the microdomains [see Fig. 2(bi)]. The other is along the [013] axis which has a 45° angle with respect to the Cu-O planes in both microdomains [see Fig. 2(bii)]. J_c peaks were observed at $\theta=0°$ and 180° in both cases. The peak-to-valley ratio of J_c, however, is much higher in the former (~ 2.1) than that of the latter (~ 1.4). As J is along the c or b axis, direct application of the intrinsic-pinning model shows a good fit [Fig. 2(bi), solid line]. The fit is poor when J has an angle with respect to the Cu-O planes [Fig. 2(bii), solid line].

The anisotropy of J_c is quite different in (113)-oriented YBCO thin films [Fig. 2(c)]. From a structural point of view, there exist three different types of microdomains in which the Cu-O planes have different orientations, or the c axis is aligned to the [100], [010], and [001] axes of the $SrTiO_2$ substrate, respectively. We label them as group I, II, and III. When J is along the [1$\bar{1}$0] axis [Fig. 2(ci), inset], two groups of J_c peaks are visible: the higher peaks near $\theta=35°$ and $-145°$ and the lower peaks, around $\theta=125°$ and $-55°$. Comparing this with the calculated angles of the intrinsic pinning from three different groups of Cu-O planes, we determined that the higher J_c peaks are induced by the intrinsic pinning from group III Cu-O planes and the lower peaks, from groups I and II together. When H is along $\theta=35°$ or $-145°$, a simple calculation shows that the Lorentz forces are parallel to the c axis of group III Cu-O planes where it experiences the maximum of the intrinsic pinning. At 125° and $-55°$, there exist minimum angles of 45° between the Lorentz force and both c axes of groups I and II Cu-O planes. It explains the lower peak height in this case. When J flows along the [11$\bar{6}$] axis [Fig. 2(cii)], which is perpendicular to the [1$\bar{1}$0] axis, we observed six peaks located near $\theta=\pm 23°$, $\pm 90°$, and $\pm 157°$. The calculation shows that

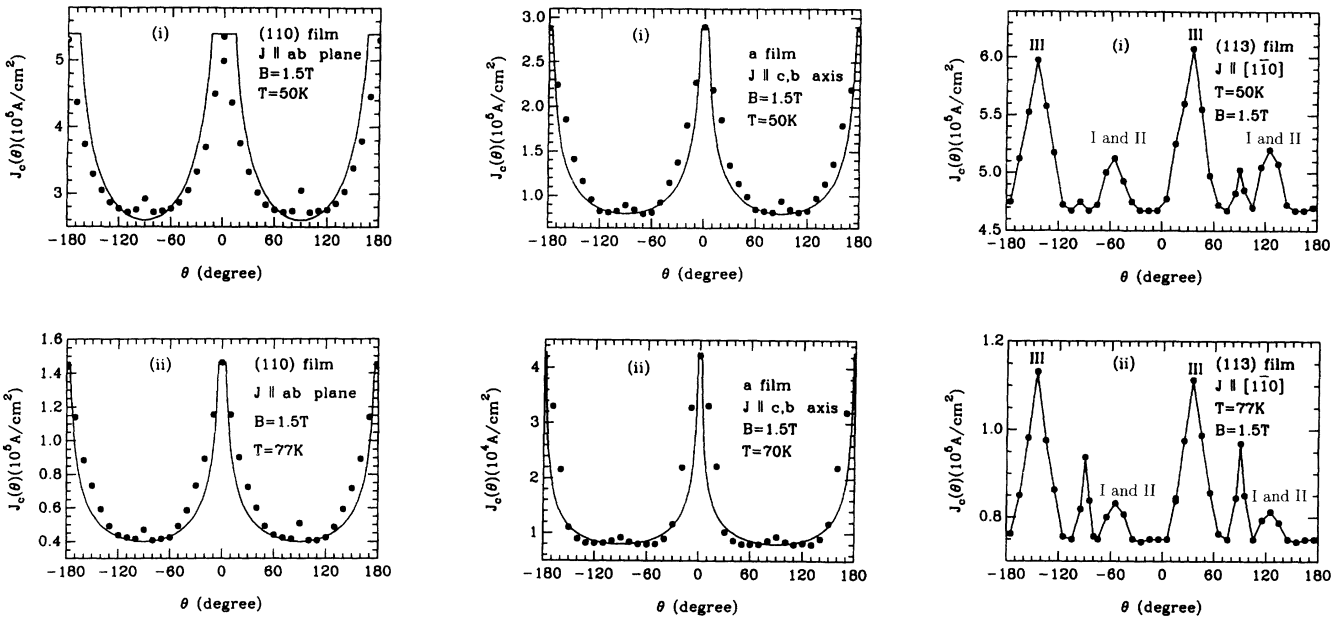

FIG. 3. High-temperature data. (a) (110)-oriented thin films as J is along the ab plane at (i) 50 K and (ii) 77 K; (b) a-axis-oriented thin films as J is along the c or b axis at (i) 50 K and (ii) 70 K; and (c) (113)-oriented thin films as J is along the [1$\bar{1}$0] axis at (i) 50 K and (ii) 77 K. Solid line in (a) and (b) is the fit of the intrinsic-pinning model. The field is 1.5 T.

the peaks at 23° or −157° are due to group I, and the peaks at −23° or 157°, to group II Cu-O planes. The angle between the Lorentz force and the corresponding c axis is 23.09°. J_c peaks at ±90° are contributed by group III Cu-O planes where the Lorentz force has an angle of 25.24° with respect to the c axis of group III planes. This explains the overall low value of the peak-to-valley ratio in this case.

$J_c(\theta)$'s of these samples show basically the same features at higher T's as shown in Fig. 3. Generally, the peak-to-valley ratio of the J_c due to intrinsic-pinning increases with T and the width of the peaks are getting narrower. The fitting of the experimental data by the intrinsic-pinning model is fairly good at high T's for both (110)- and a-axis-oriented thin films [Figs. 3(a) and 3(b)]. It should be noticed that the width of the measured J_c peaks is narrower than that predicted by the intrinsic-pinning model at low T's but the order is reversed at high T's. It is possible that the contribution of other pinning effects, which are not considered in the intrinsic-pinning model, increases with T. For example, twin-boundary pinning was seen as broad J_c maxima only at high T's in c-axis-oriented YBCO thin films.[4] In (110)- and a-axis-oriented YBCO thin films, there are also many planar growth defects parallel to the Cu-O planes. The $J_c(\theta)$ at high T cannot be determined by intrinsic pinning only. One may also attribute the discrepancy between theory and experiment to the enhanced thermally activated flux creep[10] at high T's. When flux creep becomes non-negligible, the measured J_c may be significantly reduced. Moreover, the influence of flux creep on the value of J_c is anisotropic because of the anisotropy of the pinning effect. On the c-axis-oriented YBCO thin films,[4] a continuous transition from flux flow to flux creep was observed as H was rotated from $H\perp c$ axis to $H\|c$ axis position. A similar phenomenon has also been observed in our (110)- and a-axis-oriented thin films.

Besides the J_c peak discussed above, a pair of J_c peaks becomes visible at $\theta=\pm 90°$ despite the orientation of the film. It should be noted that these peaks were not seen at low T (Fig. 2) so the impurity effect, e.g., the c-axis-oriented grains in a-axis-oriented films, should be excluded as a possible case. Planar growth defects parallel to the surface could be a reason but they are unlikely to have formed in (113)-oriented thin films. In the many samples we have measured, only those with a very smooth surface show these peaks, suggesting that these peaks are caused by surface and the film-substrate interface pinning effect. The absence of this effect at low T could be attributed to the extremely short coherence length of YBCO. We will elaborate our results on surface pinning in a separate paper.[11]

B. Temperature dependence

To obtain some physical insight, the T dependence of J_c was measured at different H and θ. In Ref. 3, we reported $J_c(T)$ of (110)-oriented YBCO thin films at zero field and suggested vortex-glass behavior along the ab plane and Josephson tunnel-junction behavior along the c axis. As the magnetic field is applied either parallel or perpendicular to the ab plane, $J_c(T)$ along the ab plane shows an almost parallel shift down with respect to the zero-field curve in the low-T range [Fig. 4(a)]. This suggests the vortex-glass behavior in the ab plane. The gaps between the zero field and the nonzero field $J_c(T)$ curves

increased as T approaches T_c. $J_c(T)$ measured with H perpendicular to the ab plane decreases faster than that with H parallel to the ab plane. This may relate to the higher rate of thermally activated flux creep in the former case because of the weaker pinning. $J_c(T)$ [and $J_c(H)$] along the c axis of (110)-oriented YBCO films in the presence of a magnetic field is still under investigation and the result will be reported elsewhere. $J_c(T)$ of YBCO a-axis- and (113)-oriented thin films is shown in Figs. 4(b) and 4(c), respectively. A similar exponential decrease of J_c in the low-T region appears even though J has different angles with respect to the Cu-O planes in these thin films. It implies that the J_c's in these samples are primarily determined by the weak links between different grains. The situation may be completely different when J is along the c axis where the intragrain J_c could be even smaller, so that tunnel-junction behavior due to the layered structure of YBCO becomes dominant.[3]

C. Field dependence

$J_c(H)$'s in (110)-, a-axis-, and (113)-oriented YBCO thin films are plotted in Fig. 5 as functions of T and θ. In

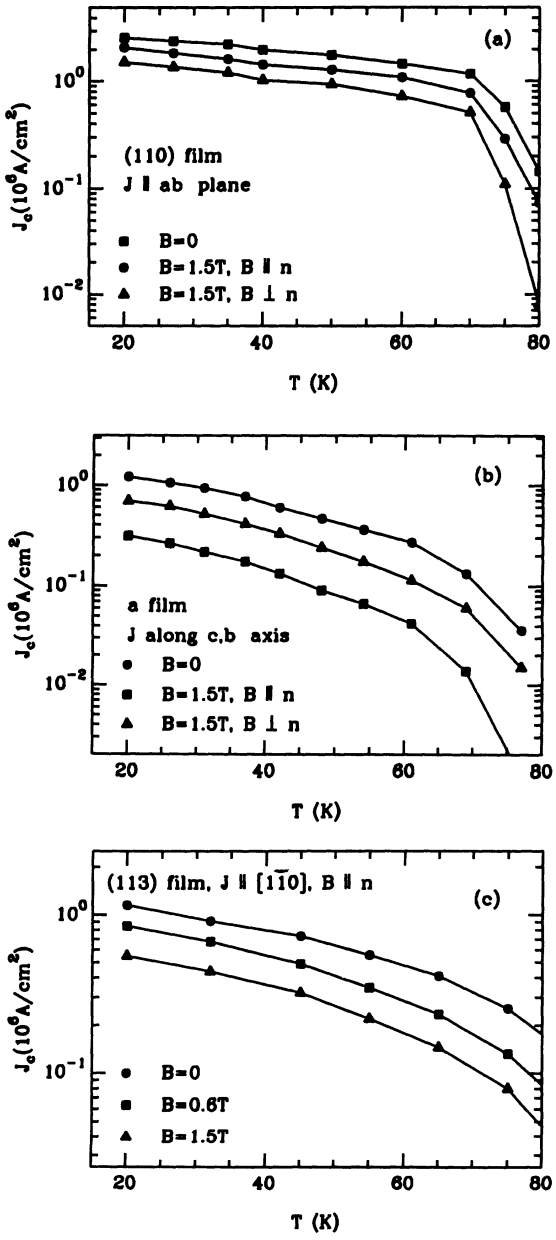

FIG. 4. $J_c(T)$ of YBCO thin films. (a) (110)-oriented thin films as J is along the ab plane, (b) a-axis-oriented thin films as J is along the c axis or b axis, and (c) (113)-oriented thin films as J is along [1$\bar{1}$0] axis.

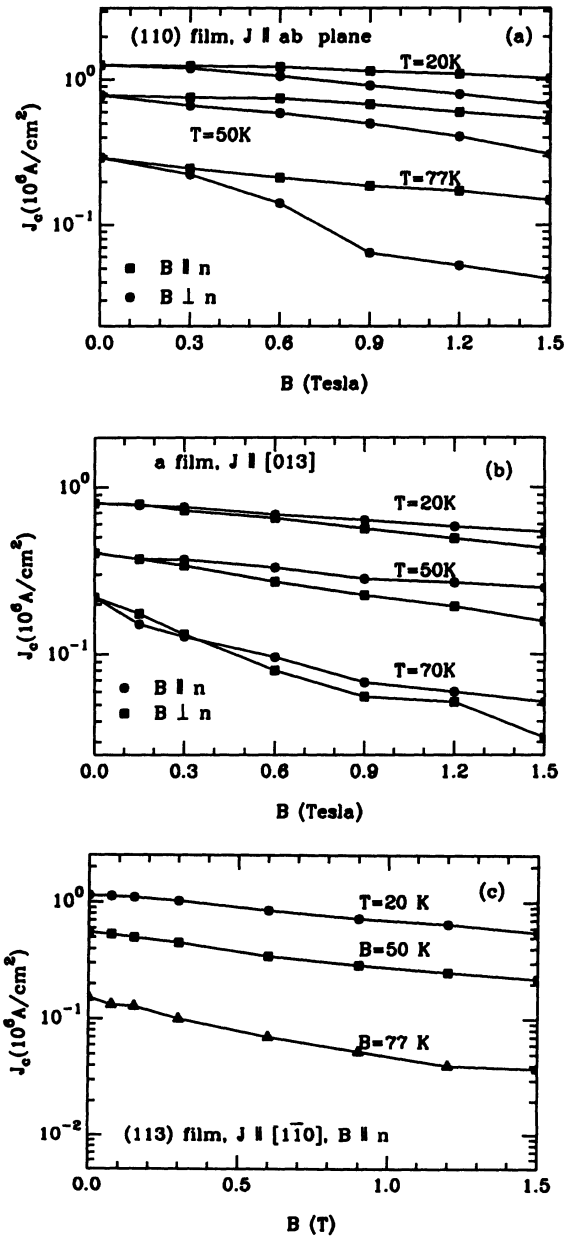

FIG. 5. $J_c(B)$ of YBCO thin films at various temperatures. (a) (110)-oriented thin films, J is along the ab plane, (b) a-axis-oriented thin films, J is along [013] axis, and (c) (113)-oriented thin films, J is along [1$\bar{1}$0] axis.

the (110)- and a-axis-oriented thin films, J is along the ab plane, while in (113)-oriented thin films, J is along the $[1\bar{1}0]$ axis. Generally, J_c in all three kinds of thin films shows weaker H dependence in the low-T region and stronger H dependence in the high-T region. The decrease of J_c with field when H is parallel to the ab plane indicates that weak layers between the Cu-O planes of YBCO are not completely transparent to the magnetic field. It implies that even though superconductivity can exist in one unit cell of YBCO, a thicker layer (along the c axis) of YBCO has a higher T_c due to weak interlayer pair interaction. The faster decrease of J_c with field at higher T's is most probably due to thermally activated flux creep. Figures 5(a) and 5(b) show that the $J_c(H)$ is anisotropic with respect to the direction of the applied field. J_c declines faster when H is perpendicular to the Cu-O planes than when H is parallel to the Cu-O planes. We understand it to be a result of the anisotropy of pinning effects. The difference of J_c between these two field configurations becomes complicated at high T's. On c-axis- (Ref. 4) and a-axis-oriented thin films [Fig. 5(b)], a crossover of the two curves was observed. Instead of going directly to zero, $J_c(B)$ in both a-axis- (at 70 K) and (110)-oriented thin films (at 77 K) shows a finite value following a sharp drop as H is parallel to the thin films. The comparison of these curves with measurements on conventional superconductors[12,13] leads one to believe that this anomaly is induced by the surface pinning effect.[11]

IV. CONCLUSIONS

We have measured the anisotropy of transport J_c in (110)-, (113)-, and a-axis-oriented YBCO thin films at various T's and H's. The experimental results indicate: (1) The dominant pinning effect is the intrinsic pinning between the Cu-O planes which is responsible for the anisotropy of the $J_c(\theta)$ despite the orientation of the film. The anisotropic $J_c(\theta)$ of (110)- and a-axis-oriented thin films agrees well with the intrinsic-pinning model when J is along the Cu-O planes. (2) The surface pinning effect has been seen only in the high-T region which is possibly the result of the extremely short coherence length of YBCO. J_c anisotropy induced by growth-defect pinning is not visible.

ACKNOWLEDGMENTS

We thank V. Selvamanickam, C. Patsinevelos, D. Lee, and K. Salama for discussions. This work was supported in part by DARPA and the state of Texas.

[1]D. K. Christen *et al.* (unpublished).
[2]K. Watanabe *et al.*, J. Appl. Phys. **3**, 1543 (1991).
[3]J. Z. Wu and W. K. Chu, Philos. Mag. B **67**, 587 (1993).
[4]B. Roas, L. Schultz, and G. Saemann-Ischenko, Phys. Rev. Lett. **64**, 479 (1990).
[5]W. E. Lawrence and S. Doniach, *Proceedings of Twelfth International Conference on Low Temperature Physics,* edited by E. Kanda (Keigaku, Tokyo, 1971), p. 361.
[6]M. Tachiki and S. Takahashi, Solid State Commun. **70**, 291 (1989); **72**, 1083 (1989).
[7]V. Selvamanickam, K. Forster, and K. Salama, Physica C **178**, 147 (1991).
[8]J. Z. Wu *et al.*, Phys. Rev. B **44**, 12 643 (1991).
[9]A. Inam *et al.*, Appl. Phys. Lett. **57**, 2484 (1990).
[10]P. W. Anderson, Phys. Rev. Lett. **9**, 309 (1962).
[11]J. Z. Wu and W. K. Chu (unpublished).
[12]M. P. A. Fisher, Phys. Rev. Lett. **62**, 1415 (1989).
[13]W. F. Druyvesteyn, D. J. van Ooijen, and T. J. Berden, Rev. Mod. Phys. **36**, 58 (1964).